

SEPARATING COMPONENTS OF THE HYSTERESIS LOSS OF NON-ORIENTED ELECTRICAL STEELS

F.J.G. Landgraf¹, J.C. Teixeira¹, M. Emura¹, M.F. de Campos², C.S. Muranaka²

¹ IPT, Instituto de Pesquisas Tecnológicas do Estado de São Paulo,
Av. Prof. Almeida Prado 532, 05508-901, Sao Paulo, Brazil, landgraf@ipt.br

² USP – Universidade de São Paulo,
São Paulo, Brazil

key words: electrical steels; magnetic losses; hysteresis loss; grain size; texture

Abstract

This paper shows that the separation of quasi-static hysteresis losses into two components, one related to Low Induction and other to High Induction levels. The separation line between those two regions has been arbitrarily chosen as the induction at maximum permeability. Results show that the grain size has stronger effect on the low induction component, while the high induction component is more sensitive to sample measuring direction. This may provide basis for better materials-properties correlation modeling and product development.

Introduction

In 1995, the world market for electrical steels has been estimated in 1.8 billion dollars [1]. Non-oriented electrical steels are widely used for the stators and rotors of rotating electrical machines. For those applications, where there is an ever-increasing demand for higher energy efficiency, new grades of steels are developed every year, offering lower magnetic losses and higher magnetic permeability [2].

There is much to be profited by the use of magnetic losses components separation for the development of electrical steels. It is now common practice to separate the magnetic losses into hysteresis, eddy-current and anomalous (or excess) components [3, 4, 5, 6, 7, 8, 9]. Based on that approach, it should be possible to identify the effects of chemical composition and microstructure in each of those components, providing a basis for better materials-properties correlation modeling and product development.

Two of the most investigated microstructural variables for electrical steels are grain size [4, 6, 10, 11, 12, 13] and texture [11, 14, 15, 16]. Increasing the grain size (G.S.) decreases hysteresis loss and increases anomalous loss, not affecting the classical eddy-current loss. Loss and permeability anisotropy are usually attributed to texture but, as it cannot be described by just one parameter, rather qualitative approaches have been used to correlate it with hysteresis and anomalous losses.

Various papers have described the ideal texture for non-oriented steels as the fibre texture $\langle 001 \rangle // ND$, based on its effect on permeability. For example, a theoretical limit for the isotropic B_{50} value of a material with that texture has been predicted as 1.85T. On the other hand, no predictions were made about the loss value of those materials, due to a lack of suitable models. We are not yet able to predict how far can the Total Magnetic Loss be lowered by texture control, for example, in a 0.5%Si steel, 0.5mm thick, that normally shows 6.0W/kg at 1.5T, 60Hz (4.7W/kg at 50Hz).

This paper proposes a methodology for the separation of the hysteresis loss component in two parts, one related to low induction and other to high induction, and discusses the results obtained in samples with different grain sizes, measured in the rolling and in the transverse direction. It is hoped that this methodology may lead to a better materials-properties correlation modeling.

Materials and methods

A low-carbon 0.5%Si steel was cast into a 50x350x300mm ingot, hot rolled to 2.5mm thickness, 350mm wide, cold rolled to about 0.55mm thickness, annealed to average grain size of 13 μ m, and subjected to several temper rolling elongations. 30x300mm Epstein samples were cut in the rolling and transverse directions and all samples were submitted to a typical industrial decarburizing annealing at 760°C for 2h. Due to different temper rolling elongation, six samples with different grain sizes and crystallographic textures were produced.

Core Loss measurements at 60Hz were performed separately in the rolling direction (RD) and transverse direction (TD) samples, with an instrument built in our lab, capable of measuring losses at frequencies from 100 to 0.01Hz, under sinusoidal induction. Total magnetic losses were measured by the wattmeter method; classical parasitic losses were calculated using electrical resistivity measured in each sample (average 19 $\mu\Omega$ cm). Hysteresis loss at 1.5T was measured by the quasi-static method, integrating the 0.01Hz hysteresis loop area. Anomalous losses were calculated from total, hysteresis and parasitic losses. Coercive force was also measured from the hysteresis loop. B_{50} values were determined at 60Hz.

The method for separation of hysteresis loss component into a low induction and high induction component will be described below.

Results and discussion

The annealing of samples with temper rolling in the range from 0 to 17% elongation resulted in grain sizes from 13 to 360 μ m. The sample with 4% elongation showed some inhomogeneities in the grain size distribution. No texture measurements were attempted in the samples with grain size larger than 50 μ m. An ODF- Orientation Distribution Function analysis of the 13 μ m sample texture showed a $\{111\}\langle uvw \rangle$ fiber component (average 3.5 times random) and a Goss component reaching 1.8 times random. Assuming that the B_{50} value is strongly dependent on the texture, its measurement in the rolling and transverse direction should offer an idea of the texture evolution with grain size. From the B_{50} values of Table 1 we may assume that a larger Goss component could be present in the 48 to 163 μ m samples, and a larger $\{111\}\langle uvw \rangle$ fraction at the 360 μ m sample.

Table 1. Effect of prior temper rolling elongation on grain size, Induction at 5000 A/m (B_{50}) in the Rolling (RD) and Transverse (TD) direction of annealed samples.

elongation	%	0	17	13	11	7	4
G.S.	(μm)	13	48	104	125	163	360
B_{50} (RD)	(T)	1.75	1.75	1.75	1.75	1.77	1.71
B_{50} (TD)	(T)	1.75	1.70	1.68	1.68	1.68	1.67

The effect of grain size on the losses components can be seen in Figure 1. Hysteresis loss decreases and anomalous loss increases when grain size is increased, as expected from literature, except in the 13 μm sample, where anomalous loss is high, for unknown reason. It is also possible to see that the anisotropy of the Total Magnetic Losses can be attributed to the anisotropy of hysteresis loss, as the anomalous component shows very little anisotropy. Hysteresis losses at the transverse direction are from 12 to 36% higher than in the rolling direction.

The anisotropy of the hysteresis loss can be seen when the shapes of hysteresis loops in the two different directions of the same sample are compared, as in Figure 2. There we may see that, although the coercive force is slightly larger in the transverse direction (10% larger, on the average), loop area is 20% larger (on the average) in the transverse direction. We will see below that most of the loss difference is concentrated in region above maximum permeability.

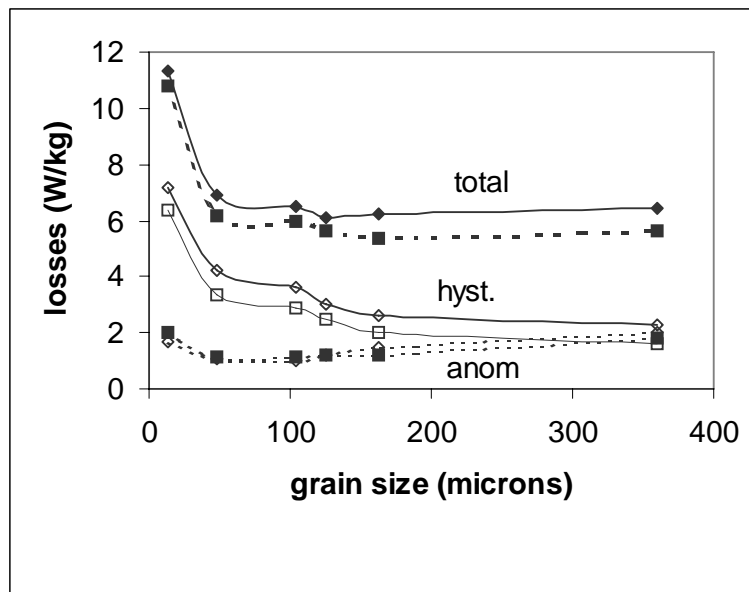


Figure 1. Effect of grain size on Total Magnetic Losses, Hysteresis Loss and Anomalous Loss at 1.5T 60Hz, measured in the Rolling direction (\square) and Transverse Direction (\diamond).

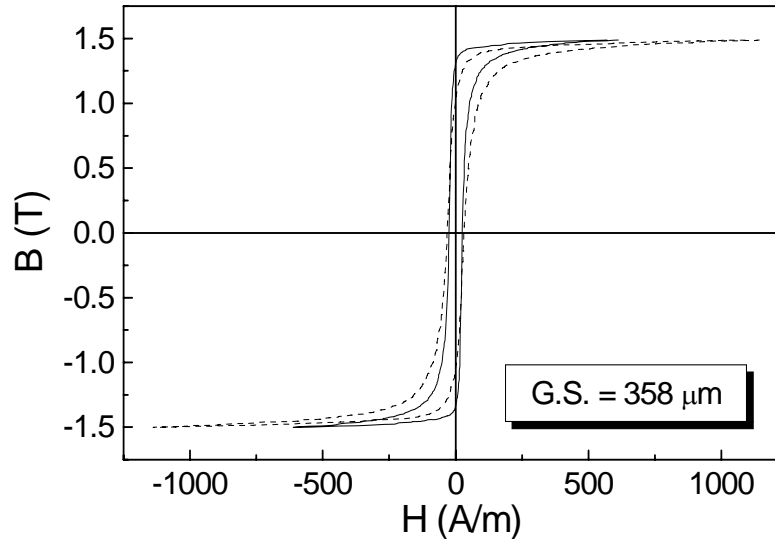


Figure 2. Hysteresis loops of the sample with grain size of 358 μm , measured on the rolling (full line) and transverse direction (dotted line)

We have also observed that, in most cases, the initial magnetization curve joins the lower branch of the hysteresis loop just below the point of maximum permeability, which is about the position of the “knee” of the hysteresis loop. This “knee” of the curves is usually associated with a change in the magnetization mechanism, suggesting that the hysteresis loss can be separated in two components: a low induction (LI) and a high induction (HI) component.

We found no better indicator for a line to separate magnetization mechanisms regions than the maximum permeability point. Figure 3 gives the impression that the knee of the curve lies above the maximum permeability point, but the visual impression of the knee position changes with the x-scale used. The values of the Low Induction and High Induction components discussed below were calculated from the integration of the areas inside and outside the maximum permeability induction lines, as exemplified in Figure 3.

Figure 4 shows the effect of grain size on the energy per cycle values of the two components, in the rolling and transverse direction. It can be seen that, as grain size is increased, the Low Induction (LI) component is reduced from 600 to 100J/m³, and the High Induction (HI) component falls from 300 to 150J/m³. Besides that, it can also be seen that there is not much anisotropy in the LI component and a large anisotropy in the HI component. In all samples, more than 50% of the Total Loss anisotropy is due to the HI component anisotropy. As an example, the 54J/m³ difference in the HI component of the 358 μm sample, seen in figure 4, accounts for 50% of its total Magnetic Loss anisotropy of 0.8W/kg, seen in figure 1.

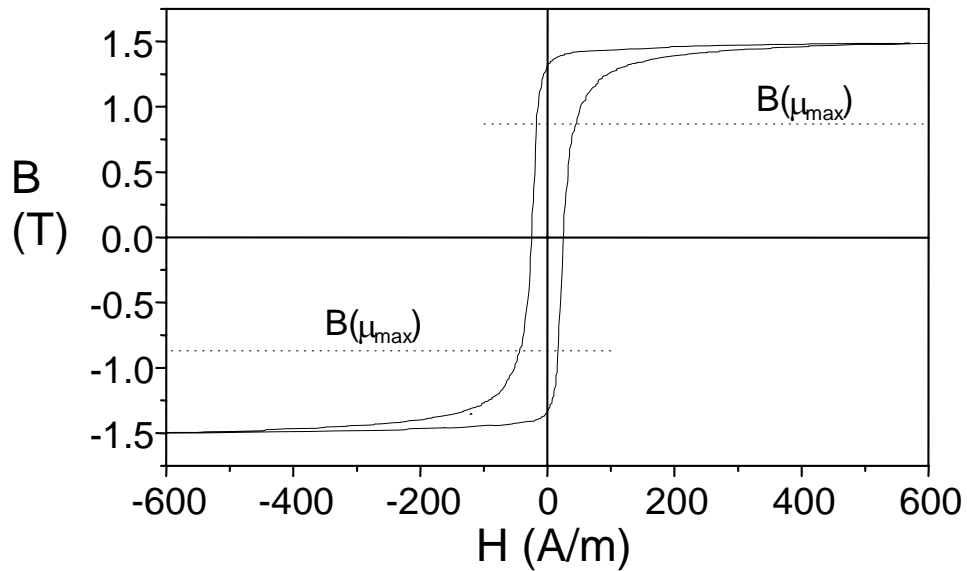


Figure 3. Hysteresis loop of the 358µm sample, rolling direction, showing the position of the maximum permeability induction.

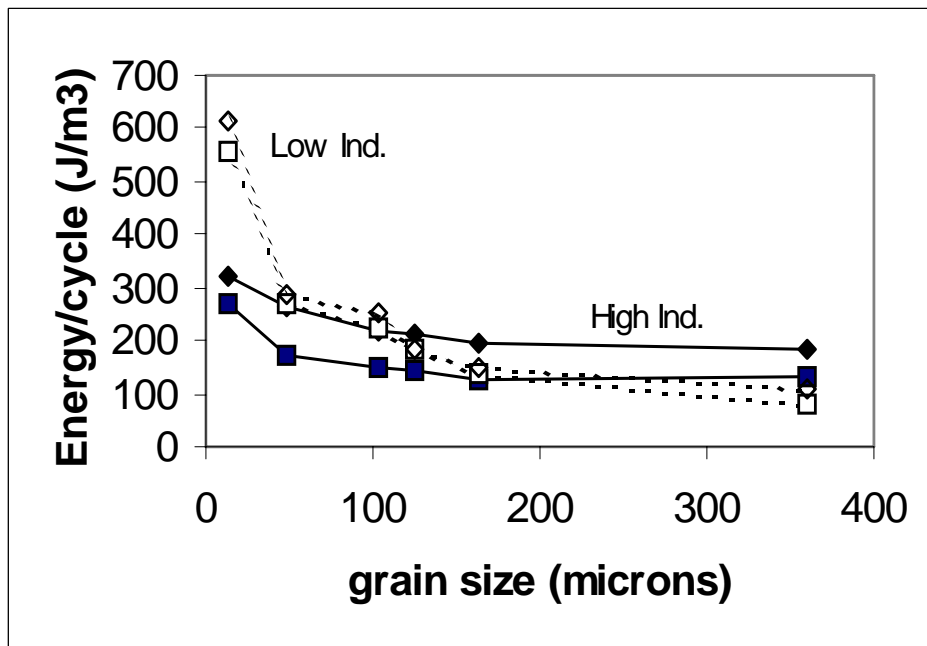


Figure 4. Effect of grain size on the Energy Loss / cycle in the Low Induction component (dotted line) and in the High Induction component (full line), measured in the Rolling direction (□) and Transverse Direction (◇).

It is normally assumed that the anisotropy of Losses and B_{50} are due to texture. Nevertheless, it was not possible to correlate the High Induction component values with B_{50} values. For example, the large decrease in B_{50} value found in the 358 μm rolling direction sample is not matched by a related increase in the HI component value.

Classical textbooks [17,18] state that the induction at the knee of the magnetization curve divides regions of different predominant magnetization behavior: below the knee, domain wall movement is the main magnetization process, whether domain rotation dominates above it. Although it is probably true that domain wall movement is the main mechanism for losses in the Low Induction region, we have refrained to use Domain Rotation as the main mechanism for the High Induction region losses. The text books assume the reversible domain rotation as the main mechanism above the knee, and reversible changes do not generate losses.

True Reversible Rotation is what occurs in the upper branch of the loop, from Maximum Induction to Remanence or to the “knee” of the upper branch. Chikazumi also mentions the existence of large Barkhausen jumps above the knee of the curve of the lower branch. He attributes those jumps to domain wall displacement and/or irreversible domain rotation, but states that “irreversible rotation is expected in fine particles or in an extremely heterogeneous materials which contains a lot of inclusions and precipitates”, which is not the case of the samples here investigated.

So, it is still open for discussion which is the predominant mechanism of energy dissipation in the high induction range of the hysteresis loss of electrical steels, whether irreversible rotation or domain wall movement. Whichever is the prevalent mechanism, it should be more sensitive to sample direction, to explain the strong anisotropy of the High Induction Losses.

Conclusions

A methodology for separating the hysteresis loss component into a High Induction and a Low Induction component is proposed, using the maximum permeability induction line to separate the two regions. This procedure may be useful, based on the observation that a significant amount of the hysteresis loss is dissipated in the High Induction region, and this component is very sensitive to texture.

Based on that methodology, it is possible to show that grain size increase lowers much more the Low Induction component, and that most of the Total Magnetic Loss anisotropy can be attributed to the High Induction component.

Acknowledgements

Thanks to FAPESP (proc. 97/4877-0) and CSN for the research grant, Flavio Beneduce Neto for ingot casting, Saturnino Ltd for the hot and cold rolling, Quantech for the temper rolling, Tempel Ltd for the industrial heat treatment.

References

- [1] T. Abraham, T. - Soft Magnetic Materials'96, Gorham/Intertech Consulting, 1996
- [2] A. Hiura ; Y. Oda ; Y. Tanaka ; S. Kazama ; Y. Okami , NKK Tech. Review 77 (1997) p. 27-33

- [3] K. Eloot, J. Penning, J. Dilewijns , Journal De Physique, to be published

- [4] F. Fiorillo, E. Ferrara, L. Ferrando, C. Appino, C. Lebourg, J. Degauque, M. Baricco,. IEEE Trans. Mag. 33 (1997) p. 3802-3804.

- [5] A.D. Paepe, K. Eloot, J. Dilewijns, C. Standaert, JMMM 160 (1996) P. 129-130.

- [6] C.K. Hou, IEEE Trans. Mag., 32 (1996) p. 471-477.

- [7] B. Cornut, A. Kedous-Lebouc, T. Waeckerlé JMMM 160 (1996) p. 102-108.

- [8] J.C.Bavay, J. Verdun, J. Materials Eng. Performance 2 (1993) p. 169-172.

- [9] G. Bertotti, , J. Appl. Phys. 57 (1985) p. 2110-2117.

- [10] M. Shiozaki, Y. Kurosaki, J. Mat. Eng. 11 (1989) p. 37-43.

- [11] E.T. Stephenson, M.R. Amann, Energy Efficient Electrical Steels, 1980.

- [12] J. Degauque, B. Astie, J.L. Porteseil, R.Vergne, JMMM 26 (1982) p. 261-263.

- [13] G. Bertotti, G.D. Schino, A.F. Milone, F. Fiorillo, J. de Physique 9 (1985) p. 385-388.

- [14] H. Shimanaka, K. Matsumura, T. Irie, H. Nakamura, JMMM 19 (1980) p. 63-64.

- [15] G.H. Shirkoohi, A.J. Moses, JMMM 133 (1994) p. 440-442, 1994.

- [16] G. Bertotti, G. Ban, G. Abbruzzese, J. Appl. Phys. 73 (1993) p. 6612-6614.

- [17] R.M. Bozorth, Ferromagnetism, Van Nostrand, 1951, p. 480

- [18] S. Chikazumi, S. Physics Of Magnetism, J.Wiley, 1964, P. 245